Trends in the Activation of Light Alkanes on Transition Metal Surfaces

Journal:	*The Journal of Physical Chemistry*
Manuscript ID	jp-2020-080766.R1
Manuscript Type:	Article
Date Submitted by the Author:	n/a
Complete List of Authors:	Araujo-Lopez, Eduard; Karlsruher Institut fur Technologie, IKFT Vandegehuchte, Bart; Total Research & Technology Feluy Curulla-Ferre, Daniel; Total Raffinage-Chimie Sharapa, Dmitry; Friedrich-Alexander-Universitat Erlangen-Nurnberg, Institute of Catalysis Research and Technology (IKFT) Studt, Felix; Karlsruher Institut für Technologie, Institute of Catalysis Research and Technology

Trends in the Activation of Light Alkanes on Transition Metal Surfaces

Eduard Araujo-Lopez,† Bart D. Vandegehuchte,§ Daniel Curulla-Ferré,§ Dmitry I. Sharapa,† and Felix Studt,†,‡*

† Institute of Catalysis Research and Technology, Karlsruhe Institute of Technology, Hermann-von-Helmholtz Platz 1, 76344 Eggenstein-Leopoldshafen, Germany

§ Total Research & Technology Feluy, Zone Industrielle Feluy C, B-7181, Seneffe, Belgium

‡ Institute for Chemical Technology and Polymer Chemistry, Karlsruhe Institute of Technology, Engesserstrasse 18, 76131 Karlsruhe, Germany

ABSTRACT. The first (oxidative) dehydrogenation step of light alkanes (ethane, propane, and *n*-butane) on transition metal (closed-packed and stepped) surfaces is analyzed using DFT calculations. It is shown that the transition state energies (ΔE_{TS}) of the C-H bond activation scale linearly with the corresponding final state energies (ΔE_{FS}), and all alkanes studied here share the

same linear scaling relationships for the non-oxidative, oxygen-assisted, and hydroxyl-assisted reactions. Variations in ΔE_{TS} between alkanes can be mainly attributed to differences in dispersion contributions determined by the carbon-chain length. As the carbon chain increases, the ΔE_{TS} of the alkane C-H bond activation decreases. In addition, the ΔE_{TS} of the first (O)DH step of propane and *n*-butane are linearly correlated with the ΔE_{TS} of the first ethane (O)DH step. We also find that the oxygen and hydroxyl adsorption energies on the transition metal surfaces (closed-packed and stepped) are dictating the promoting/poisoning effect of the C-H bond activation. Based on our extensive DFT calculations, we find that Pt has the lowest C-H bond transition state energy for both the non-oxidative and the oxidative pathways, and metals such as Au and Ag become active for C-H bond activation of alkanes only when oxygen and hydroxyl species are present on the metal surfaces. Finally, by establishing scaling relationships over a wide range of transition metal surfaces, we have developed a simple and highly accurate model for the prediction of C-H bond activation barriers for the (oxidative) dehydrogenation of light alkanes.

1. INTRODUCTION

The dehydrogenation (DH) of light alkanes into alkenes has gained more attention recently due to their increased supply from the

shale gas boom.[1–3] Light alkenes are mainly used as building blocks for polymers and are typically produced by naphtha steam crackers and from fluid catalytic cracking.[4] Commercially, non-oxidative DH is already providing an alternative route to alkenes using Pt- and CrO_x-based catalysts through the so-called Olefex and Catofin processes. These technologies are used to fill the C_3 and C_4 olefins demand, while ethane DH is less pursued today due to more unfavorable thermodynamics, and an abundance of C_2 feeds on the market. The conversion of alkanes in the non-oxidative DH is limited by the production of hydrogen which shifts the thermodynamic equilibrium to the reactant side, and high temperatures are required to reach reasonable reaction rates.[5,6] On the other hand, the oxidative DH (ODH) of alkanes using O_2 or CO_2 represents an attractive option, but is still in the early stages of development with catalyst design and process economics needing improvement. The use of molecular O_2 leads to an overoxidation, a low alkene yield and a fast deactivation of the catalyst, which is still very poorly understood. However, coupling this reaction with CO_2 (as a softer oxidant) which removes hydrogen through the reverse water-gas shift (rWGS) reaction moves the reaction again to the product side, thereby increasing the alkene yield.[4,7–10] The promoting/poisoning effect of the surface O* and OH* intermediates (formed during the ODH of alkanes) play an essential role in C–H bond activation, both in the functionalization of hydrocarbons and

their partial oxidation. The first DH step herein has been shown to play a significant role as a rate-determining step.[11–17]

C-H bond activation and the DH process on transition metal (TM) surfaces have been widely investigated for light alkanes, both experimentally and theoretically. For instance, the activation of methane under moderate conditions was only observed on oxygen-pre-covered Cu surfaces, and by using DFT calculations, it was shown that the activation energy of methane is decreased by using promoters such as O*, OH*, O_2*, and OCH_3.[18–21] Promoters for methane activation have also been evaluated on Pd and Au as well as their alloys.[22,23] Alkane DH has been studied primarily on Pt catalysts for the non-oxidative process, and investigations targeted Ni and Pd for the ODH process.[10,13,32–34,24–31] The direct dissociative chemisorption of propane and *iso*-butane and their fully deuterated isotopes was studied on the Pt(110) surface, where it was found that the difference in activation energies of C-H and C-D bond cleavage can be attributed to differences in zero-point energy stemming from the two isotopes.[35–37]

The combination of explicit DFT calculations and simple modeling methods such as scaling relationships has proven to be an essential tool in the computational search for new and promising catalysts.[38–42] The scaling relationships can be viewed as the correlation between a descriptor and the transition state energy of a specific reaction,[43–49] with descriptors typically being the final state or

adsorption energies of one or a few key intermediates.[41,50,51] For the C–H bond activation and (de)hydrogenation reactions of alkanes several scaling relationships have been proposed.[11,13,58–62,31,45,52–57] One of the first attempts to generalize a set of de(hydrogenation) reactions for several reactants including methane, ethane, and propane over close-packed and stepped surfaces of TMs was proposed by Wang et al.[53] Therein, with a suitable choice of reference systems, the transition state scaling relationship was approximated to just one single linear scaling relationship (LSR). LSRs between the final state energies and the corresponding transition state energies have been used to understand the effect of co-adsorbed species on metal surfaces. For instance, it was found that the X-H bond activation (with X=C, N, O, S) does not only depend on the binding strength of the X/X-H species, but also of the H atom being extracted during X-H bond activation.[54–56,58] Based on trends observed for the C-H bond activation of methane on TMs it has been possible to understand the origin of the promoting/poisoning effect of non-metals (B, C, N, P, O, S, and Se) and to describe the C-H, N-H, and O-H bond activation across a range of reactions.[57] Other LSR studies include methane activation on single-atom alloys[61] and the C-H bond activation of the non-oxidative dehydrogenation of ethane and propane on TMs.[11,13,31,62]

For larger alkanes, the effect of co-adsorbed species such as oxygen and hydroxyl in the C-H bond activation on TMs surfaces has not been investigated in detail yet. In this paper, a systematic study of the first (oxidative) dehydrogenation step of light alkanes (ethane, propane, and *n*-butane) over close-packed and stepped TM surfaces (Scheme 1) has been performed using DFT calculations. As these (O)DH reactions can be catalyzed by a vast range of materials including noble metals and transition metal oxides, herein, the TMs most frequently used have been chosen: Ag, Au, Cu, Ni, Co, Pd, Rh, and Pt.

Scheme 1. (a) Overview of reaction pathways for the non-oxidative (green), O-assisted (blue), and OH-assisted (red) DH of alkanes, and (b) Illustration of the first (O)DH step of propane on close-packed (top) and stepped (bottom) transition metal surfaces

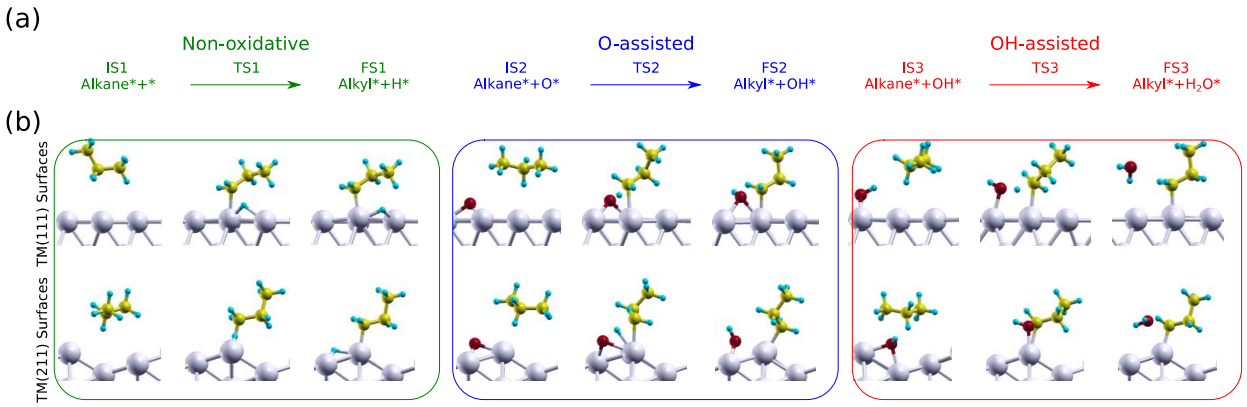

2. COMPUTATIONAL METHODS

DFT calculations were carried out using the Vienna Ab Initio Simulation Package (VASP)[63,64] and the Atomic Simulation Environment (ASE)[65] employing the generalized gradient approximation (GGA) Bayesian error estimation functional with van der Waals corrections (BEEF-vdW)[66,67] and the projector-augmented wave (PAW) potentials.[68,69] The choice of the functional is motivated by its performance regarding the description of adsorption energies[70] and transition states[71] on TM surfaces. A similar setup, as well as, the reference energy levels for the final states (FS) and the transition states (TS) of the LSR are defined as in a recent work from our group,[28] where the gas-phase molecules (ethane, propane or *n*-butane) and the TM surfaces (with or without the preadsorbed oxygen species) were taken as the reference. When specified, single-point calculations were performed using the PBE functional, including Grimme's dispersion corrections (PBE-D3) using the same parameters.[72,73] The transition state (TS) searches along the reaction path were systematically performed using the nudged elastic band (NEB)[74] and DIMER[75] methods at the same theoretical level as those for the reactants and products. A single imaginary frequency along the reaction coordinate confirmed the final TS structures, the frequencies were calculated with a normal mode analysis by using a finite-difference approximation of the Hessian matrix. Further details are given in the Supporting Information.

An analysis for validation of the statistical significance and physical meaning of the parameter estimates was performed, as explain by Toch et al.[76] The significance of every individual parameter was tested employing a *t*-test, as well as, the 95% confidence intervals (CI), mean absolute error (MAE), and maximum residual error were calculated.

3. RESULTS & DISCUSSION

Previously, we investigated the dehydrogenation of propane over Pd(111) and Pd(211) surfaces and the effect of promotion with surface oxygen and hydroxyl.[28] It was found that the transition state energies (ΔE_{TS}) scale linearly with the final state energies (ΔE_{FS}), for both the non-oxidative and the oxidative dehydrogenation steps. Herein, this analysis is extended to the first (O)DH step of ethane, propane, and *n*-butane over a range of TM surfaces.

3.1. Non-oxidative DH of Ethane on TM Surfaces

Figure 1 shows the linear relationship between the ΔE_{TS} for the first DH step of ethane following the non-oxidative pathway, and the corresponding ΔE_{FS} on several TM(111) and (211) surfaces relative to gas-phase ethane. The calculated ΔE_{TS} range from 0.37 eV (Pt) to 2.28 eV (Ag), and the energy barriers to activate the adsorbed molecules (initial state, IS) are in fair agreement with recent reports for Pt, Ni and Cu surfaces.[30–33,77–79] We observe a weak geometric effect when comparing the (111) to (211) surfaces

(with the intercepts being different by app. 0.1 eV), which is in line with other studies on dehydrogenation reactions[53,80] and also points to the reaction being rather surface insensitive (see Figure S1a for a more quantitative analysis of scaling relations).

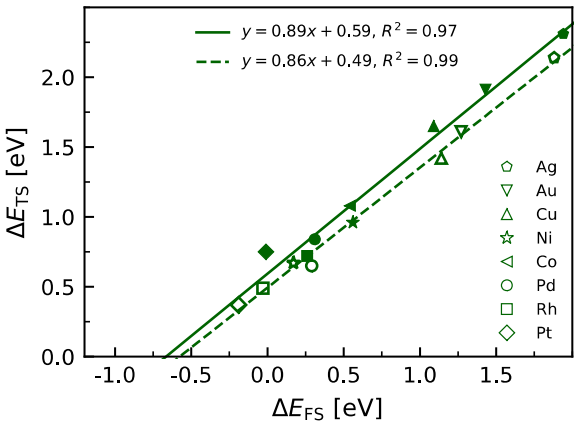

Figure 1. Transition state energies as a function of the final state energies for the non-oxidative DH of ethane on TM surfaces. Filled and open markers correspond to TM(111) and (211) surfaces, respectively.

3.2. Oxidative DH of Ethane on TM Surfaces

Transition state scaling relationships (similar to those obtained for non-oxidative DH) are observed for the oxygen and hydroxyl assisted DH of ethane, as shown in Figure 2. Overall, the results presented here for the TM(111) surfaces are in line with what has been found previously for methane activation assisted by oxygen and hydroxyl species.[54–58] For the first ODH step of ethane on O- and OH- modified surfaces, the ΔE_{TS} are directly correlated with the oxygen/hydroxide adsorption energies (Table S2 and Figure S2).

We generally find that metals that adsorb the oxygen and hydroxide species strongly, such as Co, Cu, and Ni, have higher ΔE_{TS}. For metals with weak adsorption energies such as Au, Ag (and Pt) we observe a much lower ΔE_{TS} compared to the non-oxidative pathway and hence a strong promotional effect of O* and OH* (see also Table S2 and Figure S2 for all metals).

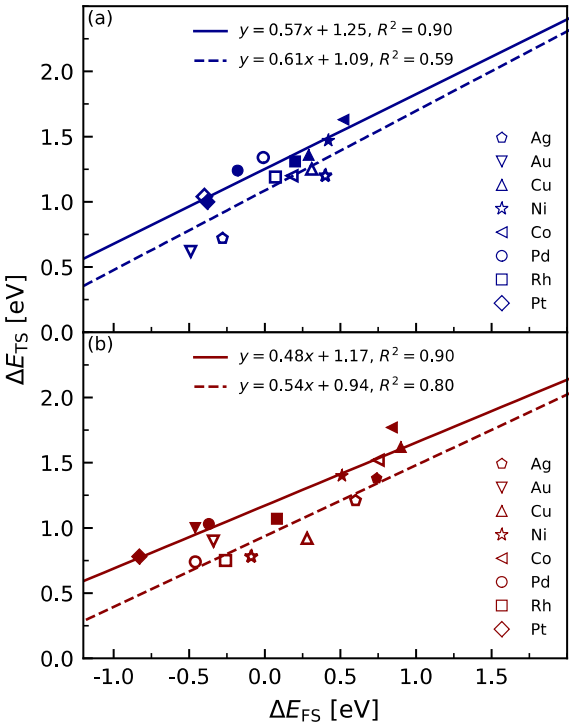

Figure 2. Transition state energies as a function of the final state energies for the (a) O- and (b) OH-assisted dehydrogenation of ethane on TM surfaces. Filled and open markers correspond to TM(111) and (211) surfaces, respectively.

Regarding the effect of undercoordinated surface sites such as steps and kinks, as can be seen in Figure S1a, the O-assisted DH on Co and Rh on the (211) surface is more favorable than on the

(111) terrace. The same effect is seen for the process with the assistance of co-adsorbed OH on Cu, Ni, Rh, and Ag. In this figure, a gray area of ±0.1 eV has been included to indicate energy differences that are below the accuracy of our calculations;[70,71,81] (among those are Ni, Cu, Pt, and Pd for O-assisted, and Pd, Co, and Au for OH-assisted). For Au(111) and Ag(111), the LSR presented in Figure 2 and the calculated ΔE_{FS} were used to determine the ΔE_{TS}, which are around 1.0 eV (Table S4), the ΔE_{TS} for the O-assisted DH of ethane on Ag and Au (211) surfaces, on the other hand, are significantly lower.

The oxygen/hydroxyl species effect on each surface can be illustrated in a similar manner by analyzing the ΔE_{TS} difference between the O-/OH-assisted and the non-oxidative DH as a function of the difference in ΔE_{FS}, as shown in Figure S1b. An inspection of Figure S1b reveals that the C-H bond activation of ethane is significantly enhanced on coinage metals (Cu, Ag, and Au) by surface oxygen and hydroxyl species on both surfaces. On Ni, Co, and Rh, the strong oxygen and hydroxide adsorption energies seem to poison the surfaces, increasing the ΔE_{TS} and the ΔE_{FS}. For those metals, dehydrogenation is more favorable in the absence of adsorbed oxygen and hydroxide adsorbed species. This effect has been showed previously by Tsai et al.[57] for methane activation, where the electronic structure of the surface and the bond order of the promoter were found to establish the trends in bond

activation. For Pd and Pt, on the other hand, the ΔE_{TS} for the O- and OH-assisted DH of ethane are higher than those for the non-oxidative DH, although the ΔE_{FS} are lower and stabilized by surface oxygen and hydroxyl species. In absolute terms, as expected from its use in commercial PDH technologies, Pt is calculated to perform best for the non-oxidative C-H bond activation of ethane, although it has quite favorable energetics for the ODH of ethane (both O- and OH-assisted) as well. From a statistical point of view, so far there is no strong motivation for the use of two separate LSRs for the (111) and (211) surfaces in each reaction pathway, because the combine LSRs for both surfaces are statistically significant (see Table S6). A detailed analysis can be found in the SI.

3.3. (O)DH of Alkanes on TM Surfaces

Next, we investigate to what extent the (O)DH of propane and *n*-butane are similar to that of ethane. Figure 3 shows the energy diagram of the first DH step of ethane, propane, and *n*-butane over the Pt(111) surface. The initial (ΔE_{IS}), transition (ΔE_{TS}), and final (ΔE_{FS}) state energies decrease as the chain length of the reactant increases in all reaction pathways; this interesting fact was pointed out before from non-oxidative DH experiments of propane and *iso*-butane on Pt(110).[35–37] In those experiments, a systematic decrease in activation energy of the DH of alkanes as well as their fully deuterated isotopes was found.

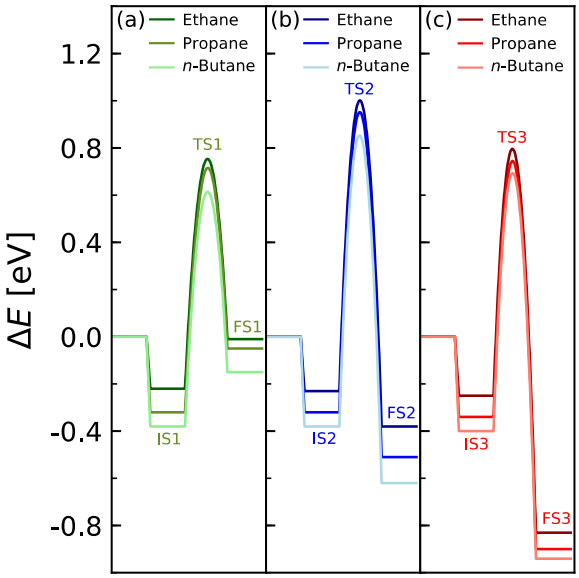

Figure 3. Potential energy diagram including initial, transition, and final states of the first dehydrogenation step of light alkanes on Pt(111) surface: (a) non-oxidative, (b) O-, and (c) OH-assisted pathways.

Table 1 shows the ΔE_{TS} of the alkane C-H bond activation and the dispersion interactions between the TS of the alkanes and the Pt(111) surface, as well as their average differences to those of ethane. The vdW forces were obtained through single-point calculations using the PBE-D3 functional and subtracting D3 contributions of surface species from those of gas-phase molecules. These calculations reveal that the D3 contributions of the TS increase as a function of the carbon-chain length, and that differences in these contributions correspond approximately to the ΔE_{TS} changes of the corresponding TS.

Table 1. Transition state energies, and differences in ZPE energy corrections and D3 contributions (with respect to the gas-phase values) for the (O)DH of alkanes on Pt(111) surface.

		Non-oxidative	O-assisted	OH-assisted	Average Diff*
Ethane	ΔE_{TS}	0.75	1.00	0.78	-
	E_{disp}	-0.56	-0.59	-0.57	-
Propane	ΔE_{TS}	0.71	0.95	0.73	-0.05
	E_{disp}	-0.62	-0.66	-0.64	-0.07
n-Butane	ΔE_{TS}	0.61	0.85	0.68	-0.13
	E_{disp}	-0.80	-0.71	-0.68	-0.16

*Differences with respect to ethane values

As the differences in the energies shown in Table 1 can mainly be ascribed to the size of the reacting molecule, one might expect a similar result for all other TM surfaces studied in this work. Indeed, this is observed in Figure 4, where the calculations are extended to propane (O)DH on TM(111) and (211) surfaces, and *n*-butane (O)DH on Pd, Cu, and Ag (111) surfaces. As shown in Figure 4a-c, the ΔE_{TS} of propane and *n*-butane are linearly correlated with the ΔE_{TS} of ethane regardless of the TM surface and promoter present (oxygen or hydroxyl). The resulting intercepts (-0.06 and -0.10

eV) are in line with the average values of the differences in ΔE_{TS} between propane/*n*-butane and ethane being -0.06 and -0.11 eV, respectively (Figure 4b-d). These values compare quite well with the average differences in dispersion contributions (the D3 part, see SI) between propane/*n*-butane and ethane, which are -0.07 and -0.19 eV. Therefore, the difference in ΔE_{TS} between alkanes is mainly attributed to their differences in dispersion contributions dictated by the carbon-chain length.

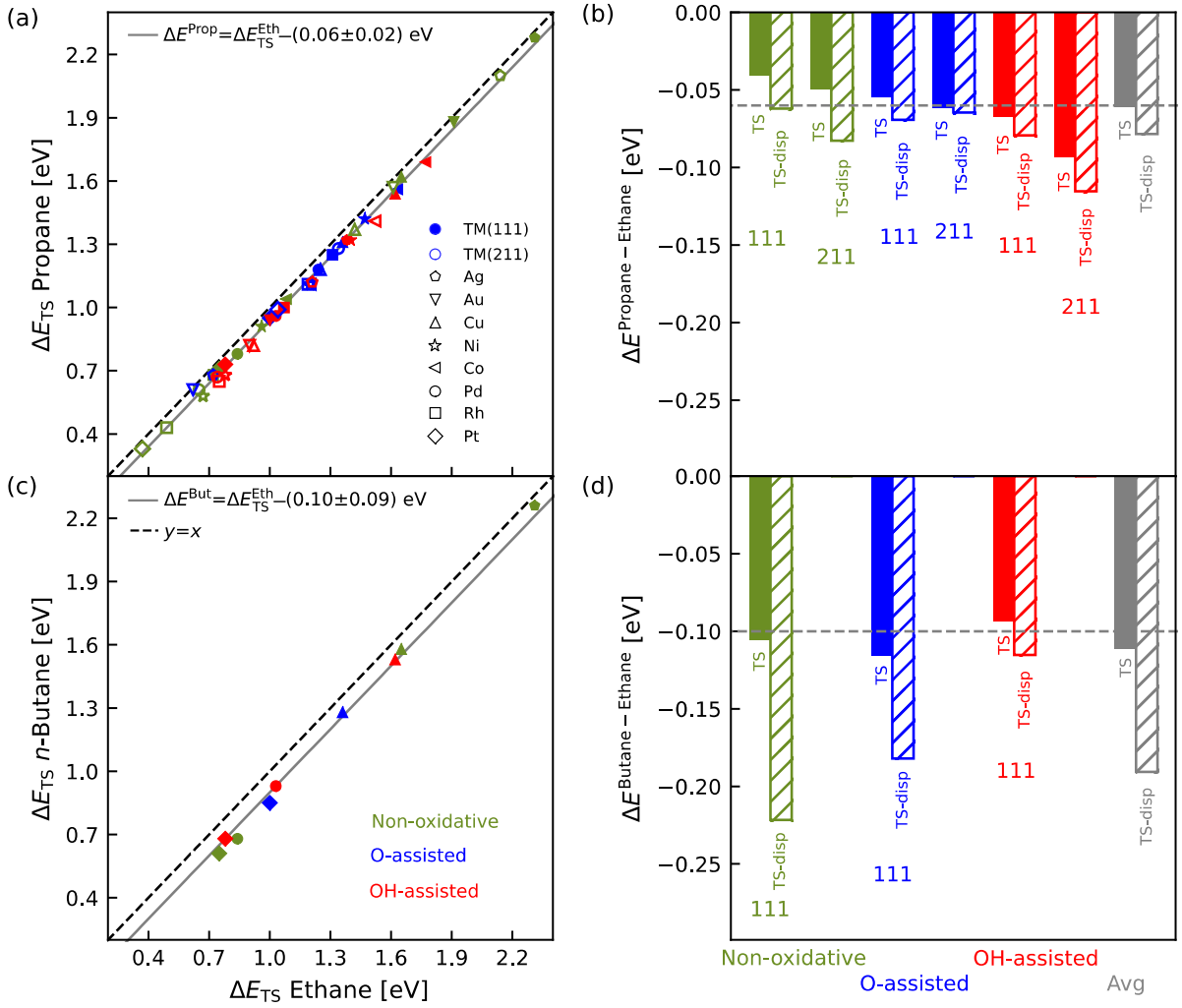

Figure 4. Linear correlation between the ΔE_{TS} of the first (O)DH steps of (a) propane-ethane and (c) *n*-butane-ethane on TM surfaces. Changes in ΔE_{TS} and dispersion contributions of the TS between (b) propane-ethane and (d) *n*-butane-ethane for the non-oxidative, O-, and OH-assisted DH on TM surfaces. The dashed lines represent the intercepts of the equations in (a) and (c). The ΔE_{TS} dispersion energy contributions data for all metals, alkanes, and reaction pathways are presented in Tables S2-S4.

The general correlations found between the ΔE_{TS} and ΔE_{FS} for all reactants and metal surfaces studied in the non-oxidative, oxygen- and hydroxyl-assisted DH are shown in Figure 5. In addition to our calculated data for ethane, propane, and *n*-butane, the values for the activation of methane on TM(111) surfaces from earlier work[56] are included. These general LSRs for alkanes are very similar to those obtained earlier for only ethane, even when a different functional (such as RPBE)[82] was used for the methane data. We rationalize this by a more or less equal shift of ΔE_{TS} and ΔE_{FS} by the dispersion contributions resulting in all data points coinciding on the same scaling line. Therefore, conclusions drawn earlier on TM surfaces and surface geometries in ethane (O)DH can be easily extended to methane, propane, and *n*-butane, showing that the C-H bond activation for each studied alkane is affected in a

similar way by surface oxygen/hydroxyl species. Importantly, the slopes of the LSR for non-oxidative DH are slightly lower than 1, while the slopes for the oxygen and hydroxyl assisted DH are all in the range of 0.5 – 0.6. This can be related to simple bond-counting arguments, with the oxygen (and hydroxyl) bond to the TM surface weakened upon abstraction of a hydrogen from the reacting alkane. The scaling relations for all (O)DH pathways were obtained across various TM surfaces and include different reactants, and could therefore be considered as predictive models for alkane C-H bond activation on metal surfaces. This is demonstrated in Figure 6 which shows a parity plot between our model based on the scaling relations from Figure 5 and the actual DFT data. Quite remarkably, the model agrees well with the DFT data leading to a MAE of only 0.08 eV. Complementarily, we have performed an in-depth statistical analysis showing the significance of established scaling relations for the full data-set. It was found that the use of individual scaling relations per surface provided a better representation of the results obtained (Table S7). A more extended discussion of the statistical analysis can be found in the SI. We therefore suggest our model for the initial screening of transition metal surfaces for alkane DH in the presence or absence of oxygen promoters.

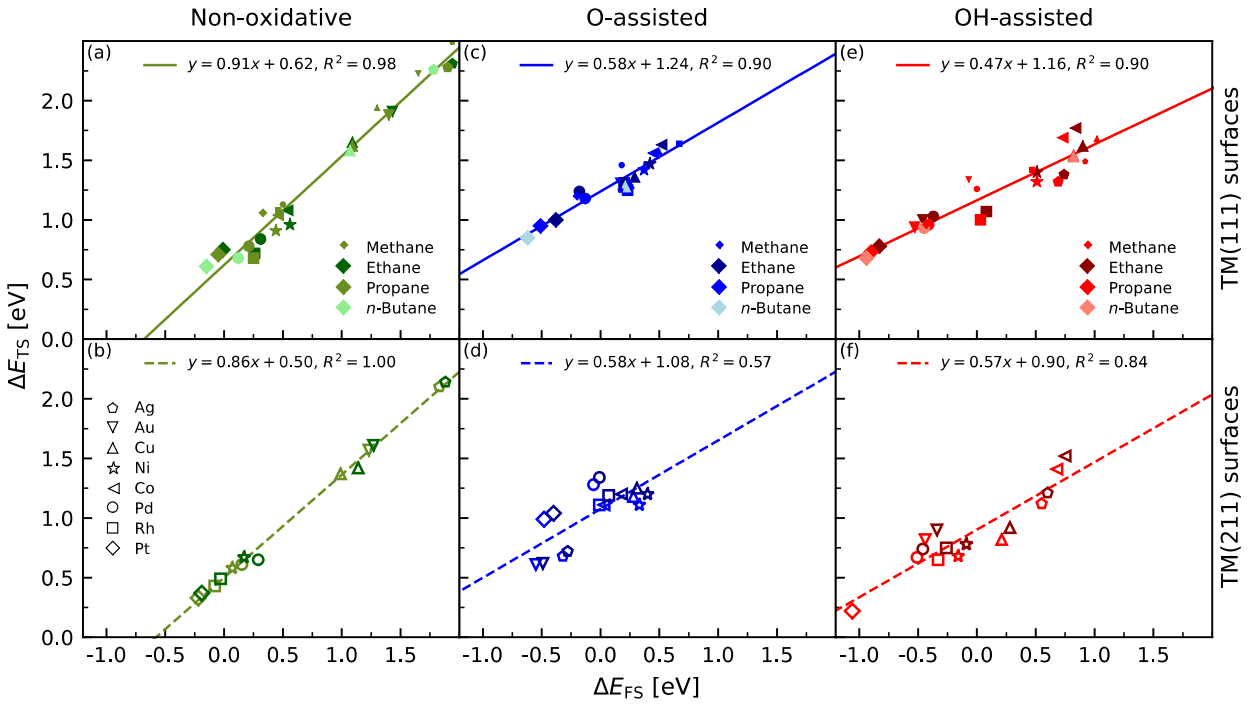

Figure 5. Transition state scaling relationships for the C–H bond activation of methane, ethane, propane, and *n*-butane for (a, b) non-oxidative, (c, d) O-, and (e, f) OH-assisted reaction pathways on transition metal surfaces. A detailed statistical analysis of the LSR is given in the SI. The data for all metals, alkanes, and reaction pathways needed to reproduce this figure are presented in Tables S3-S5. Small markers for methane activation were taken from Yoo et al.[56]

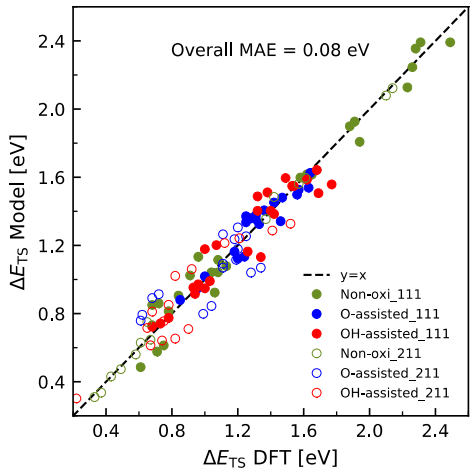

Figure 6. Parity diagram for the accuracy of the models. Calculated DFT ΔE_{TS} compared with the predictions from our models presented in Figure 5 for the (O)DH of alkanes on TM surfaces.

4. CONCLUSIONS

The first (oxidative) dehydrogenation step of light alkanes (ethane, propane, and *n*-butane) on transition metal closed-packed and stepped surfaces were analyzed using DFT calculations. It was shown that the transition state energies (ΔE_{TS}) of the C-H bond activation scale linearly with the corresponding final state energies (ΔE_{FS}), and all alkanes studied (including methane) share the same linear relationships (LSR) for the non-oxidative, O-assisted, and OH-assisted reactions. This is because the ΔE_{TS} and ΔE_{FS} of the alkanes are equally shifted by the dispersion interactions with the transition metal surfaces. Variations in ΔE_{TS} between alkanes were primarily attributed to differences in dispersion contributions determined by the carbon-chain length. As

the carbon chain increases, the ΔE_{TS} of the alkane C-H bond activation decreases. As a result, the ΔE_{TS} of the first (O)DH steps of propane and *n*-butane are linearly correlated with the ΔE_{TS} of ethane and we expect that this also applies to longer alkanes.

Our analysis also evaluated the impact of oxygen and hydroxyl adsorption on the transition metal surfaces on promoting (e.g. for Au and Ag) and poisoning (e.g. for Co, Ni and Rh) the reaction. Finally, we showed that simple models based on the LSRs are able to predict ΔE_{TS} with a remarkably small MAE for a wide range of metals, alkane reactants and DH pathways. We suggest that these LSRs are universal and can therefore pave the way towards the computational design of improved (O)DH catalysts.

ASSOCIATED CONTENT

Supporting Information. Results of the adsorption energies of oxygen species; statistical analysis; initial, transition, and final state energies; D3 contributions; coordinates of optimized structures including frequencies of the transition states

AUTHOR INFORMATION

Corresponding Author

* E-mail: felix.studt@kit.edu

Author Contributions

The manuscript was written through the contributions of all authors. All authors have approved the final version of the manuscript.

Notes

The authors declare no competing financial interests.

ACKNOWLEDGMENT

This work is part of the Consortium on Metal Nanocatalysis funded by Total Refining & Chemicals, and it was supported by the Research Program Agreement, with reference Total/IPA-5441 between Total Research & Technology Feluy and KIT.

REFERENCES

(1) Wang, Q.; Chen, X.; Jha, A. N.; Rogers, H. Natural Gas from Shale Formation – The Evolution, Evidences and Challenges of Shale Gas Revolution in United States. *Renew. Sustain. Energy Rev.* **2014**, *30*, 1–28. https://doi.org/10.1016/j.rser.2013.08.065.

(2) Wei, D.; Liu, H.; Shi, K. What Are the Key Barriers for the Further Development of Shale Gas in China? A Grey-DEMATEL Approach. *Energy Reports* **2019**, *5*, 298–304. https://doi.org/10.1016/j.egyr.2019.02.010.

(3) Plotkin, J. S. The Changing Dynamics of Olefin

Supply/Demand. *Catal. Today* **2005**, *106* (1–4), 10–14. https://doi.org/10.1016/j.cattod.2005.07.174.

(4) Gao, Y.; Neal, L.; Ding, D.; Wu, W.; Baroi, C.; Gaffney, A. M.; Li, F. Recent Advances in Intensified Ethylene Production—A Review. *ACS Catal.* **2019**, *9* (9), 8592–8621. https://doi.org/10.1021/acscatal.9b02922.

(5) Sattler, J. J. H. B.; Ruiz-Martinez, J.; Santillan-Jimenez, E.; Weckhuysen, B. M. Catalytic Dehydrogenation of Light Alkanes on Metals and Metal Oxides. *Chem. Rev.* **2014**, *114* (20), 10613–10653. https://doi.org/10.1021/cr5002436.

(6) James, O. O.; Mandal, S.; Alele, N.; Chowdhury, B.; Maity, S. Lower Alkanes Dehydrogenation: Strategies and Reaction Routes to Corresponding Alkenes. *Fuel Process. Technol.* **2016**, *149*, 239–255. https://doi.org/10.1016/j.fuproc.2016.04.016.

(7) Cavani, F.; Ballarini, N.; Cericola, A. Oxidative Dehydrogenation of Ethane and Propane: How Far from Commercial Implementation? *Catal. Today* **2007**, *127* (1–4), 113–131. https://doi.org/10.1016/j.cattod.2007.05.009.

(8) Atanga, M. A.; Rezaei, F.; Jawad, A.; Fitch, M.; Rownaghi, A. A. Oxidative Dehydrogenation of Propane to Propylene with Carbon Dioxide. *Appl. Catal. B Environ.* **2018**, *220*, 429–445.

https://doi.org/10.1016/j.apcatb.2017.08.052.

(9) Wang, S.; Zhu, Z. H. Catalytic Conversion of Alkanes to Olefins by Carbon Dioxide Oxidative Dehydrogenation - A Review. *Energy and Fuels* **2004**, *18* (4), 1126–1139. https://doi.org/10.1021/ef0340716.

(10) Nowicka, E.; Reece, C.; Althahban, S. M.; Mohammed, K. M. H.; Kondrat, S. A.; Morgan, D. J.; He, Q.; Willock, D. J.; Golunski, S.; Kiely, C. J.; et al. Elucidating the Role of CO 2 in the Soft Oxidative Dehydrogenation of Propane over Ceria-Based Catalysts. *ACS Catal.* **2018**, *8* (4), 3454–3468. https://doi.org/10.1021/acscatal.7b03805.

(11) Zha, S.; Sun, G.; Wu, T.; Zhao, J.; Zhao, Z.-J.; Gong, J. Identification of Pt-Based Catalysts for Propane Dehydrogenation via a Probability Analysis. *Chem. Sci.* **2018**, *9* (16), 3925–3931. https://doi.org/10.1039/C8SC00802G.

(12) Trinchero, A.; Hellman, A.; Grönbeck, H. Methane Oxidation over Pd and Pt Studied by DFT and Kinetic Modeling. *Surf. Sci.* **2013**, *616*, 206–213. https://doi.org/10.1016/j.susc.2013.06.014.

(13) Hansen, M. H.; Nørskov, J. K.; Bligaard, T. First Principles Micro-Kinetic Model of Catalytic Non-Oxidative Dehydrogenation of Ethane over Close-Packed Metallic Facets.

J. Catal. **2019**, *374*, 161–170. https://doi.org/10.1016/j.jcat.2019.03.034.

(14) Xiao, L.; Ma, F.; Zhu, Y.-A.; Sui, Z.-J.; Zhou, J.-H.; Zhou, X.-G.; Chen, D.; Yuan, W.-K. Improved Selectivity and Coke Resistance of Core-Shell Alloy Catalysts for Propane Dehydrogenation from First Principles and Microkinetic Analysis. *Chem. Eng. J.* **2019**, *377*, 120049. https://doi.org/10.1016/j.cej.2018.09.210.

(15) Zhao, Z.-J.; Chiu, C.; Gong, J. Molecular Understandings on the Activation of Light Hydrocarbons over Heterogeneous Catalysts. *Chem. Sci.* **2015**, *6* (8), 4403–4425. https://doi.org/10.1039/C5SC01227A.

(16) Weaver, J.; Carlsson, A.; Madix, R. J. The Adsorption and Reaction of Low Molecular Weight Alkanes on Metallic Single Crystal Surfaces. *Surf. Sci. Rep.* **2003**, *50* (4–5), 107–199. https://doi.org/10.1016/S0167-5729(03)00031-1.

(17) Niu, J.; Wang, Y.; Qi, Y.; Dam, A. H.; Wang, H.; Zhu, Y.-A.; Holmen, A.; Ran, J.; Chen, D. New Mechanism Insights into Methane Steam Reforming on Pt/Ni from DFT and Experimental Kinetic Study. *Fuel* **2020**, *266*, 117143. https://doi.org/10.1016/j.fuel.2020.117143.

(18) Alstrup, I.; Chorkendorff, I.; Ullmann, S. The

Interaction of CH4 at High Temperatures with Clean and Oxygen Precovered Cu(100). *Surf. Sci.* **1992**, *264* (1–2), 95–102. https://doi.org/10.1016/0039-6028(92)90168-6.

(19) Niu, T.; Jiang, Z.; Zhu, Y.; Zhou, G.; van Spronsen, M. A.; Tenney, S. A.; Boscoboinik, J. A.; Stacchiola, D. Oxygen-Promoted Methane Activation on Copper. *J. Phys. Chem. B* **2018**, *122* (2), 855–863. https://doi.org/10.1021/acs.jpcb.7b06956.

(20) Wang, J.; Wang, G.-C. Promotion Effect of Methane Activation on Cu(111) by the Surface-Active Oxygen Species: A Combination of DFT and ReaxFF Study. *J. Phys. Chem. C* **2018**, *122* (30), 17338–17346. https://doi.org/10.1021/acs.jpcc.8b05294.

(21) Rahmani Didar, B.; Balbuena, P. B. Methane Dehydrogenation on Cu and Ni Surfaces with Low and Moderate Oxygen Coverage. *Int. J. Quantum Chem.* **2020**, *120* (2), 1–9. https://doi.org/10.1002/qua.26065.

(22) Do, Q. K.; Tran, H.-V.; Wang, S.; Grabow, L. C. The Synergy of Dilute Pd and Surface Oxygen Species for Methane Upgrading on Au3Pd(111). *Energy Technol.* **2019**, *1900732* (111), 1900732. https://doi.org/10.1002/ente.201900732.

(23) Jiang, Z.; Wang, B.; Fang, T. Adsorption and

Dehydrogenation Mechanism of Methane on Clean and Oxygen-Covered Pd (1 0 0) Surfaces: A DFT Study. *Appl. Surf. Sci.* **2014**, *320*, 256–262. https://doi.org/10.1016/j.apsusc.2014.08.195.

(24) Yang, M. L.; Zhu, Y. A.; Fan, C.; Sui, Z. J.; Chen, D.; Zhou, X. G. DFT Study of Propane Dehydrogenation on Pt Catalyst: Effects of Step Sites. *Phys. Chem. Chem. Phys.* **2011**, *13* (8), 3257–3267. https://doi.org/10.1039/c0cp00341g.

(25) Yang, M. L.; Zhu, Y. A.; Zhou, X. G.; Sui, Z. J.; Chen, D. First-Principles Calculations of Propane Dehydrogenation over PtSn Catalysts. *ACS Catal.* **2012**, *2* (6), 1247–1258. https://doi.org/10.1021/cs300031d.

(26) Cao, X. Insight into Mechanism and Selectivity of Propane Dehydrogenation over the Pd-Doped Cu(111) Surface. *RSC Adv.* **2016**, *6* (70), 65524–65532. https://doi.org/10.1039/C6RA15038A.

(27) Gomez, E.; Kattel, S.; Yan, B.; Yao, S.; Liu, P.; Chen, J. G. Combining CO2 Reduction with Propane Oxidative Dehydrogenation over Bimetallic Catalysts. *Nat. Commun.* **2018**, *9* (1), 1398. https://doi.org/10.1038/s41467-018-03793-w.

(28) Araujo-Lopez, E.; Joos, L.; Vandegehuchte, B. D.;

Sharapa, D. I.; Studt, F. Theoretical Investigations of (Oxidative) Dehydrogenation of Propane to Propylene over Palladium Surfaces. *J. Phys. Chem. C* **2020**, *124* (5), 3171–3176. https://doi.org/10.1021/acs.jpcc.9b11424.

(29) Cai, W.; Mu, R.; Zha, S.; Sun, G.; Chen, S.; Zhao, Z.-J.; Li, H.; Tian, H.; Tang, Y.; Tao, F. (Feng); et al. Subsurface Catalysis-Mediated Selectivity of Dehydrogenation Reaction. *Sci. Adv.* **2018**, *4* (8), eaar5418. https://doi.org/10.1126/sciadv.aar5418.

(30) Myint, M.; Yan, B.; Wan, J.; Zhao, S.; Chen, J. G. Reforming and Oxidative Dehydrogenation of Ethane with CO2 as a Soft Oxidant over Bimetallic Catalysts. *J. Catal.* **2016**, *343*, 168–177. https://doi.org/10.1016/j.jcat.2016.02.004.

(31) Hook, A.; Celik, F. E. Predicting Selectivity for Ethane Dehydrogenation and Coke Formation Pathways over Model Pt–M Surface Alloys with Ab Initio and Scaling Methods. *J. Phys. Chem. C* **2017**, *121* (33), 17882–17892. https://doi.org/10.1021/acs.jpcc.7b03789.

(32) Lin, X.; Xi, Y.; Sun, J. Unraveling the Reaction Mechanism for Nickel-Catalyzed Oxidative Dehydrogenation of Ethane by DFT: The C–H Bond Activation Step and Its Following Pathways. *J. Phys. Chem. C* **2012**, *116* (5), 3503–

3516. https://doi.org/10.1021/jp2088274.

(33) Marcinkowski, M. D.; Darby, M. T.; Liu, J.; Wimble, J. M.; Lucci, F. R.; Lee, S.; Michaelides, A.; Flytzani-Stephanopoulos, M.; Stamatakis, M.; Sykes, E. C. H. Pt/Cu Single-Atom Alloys as Coke-Resistant Catalysts for Efficient C–H Activation. *Nat. Chem.* **2018**, *10* (3), 325–332. https://doi.org/10.1038/nchem.2915.

(34) Byron, C.; Bai, S.; Celik, G.; Ferrandon, M. S.; Liu, C.; Ni, C.; Mehdad, A.; Delferro, M.; Lobo, R. F.; Teplyakov, A. V. Role of Boron in Enhancing the Catalytic Performance of Supported Platinum Catalysts for the Nonoxidative Dehydrogenation of n -Butane. *ACS Catal.* **2020**, *10* (2), 1500–1510. https://doi.org/10.1021/acscatal.9b04689.

(35) Weinberg, W. H.; Sun, Y.-K. Quantification of Primary Versus Secondary C-H Bond Cleavage in Alkane Activation: Propane on Pt. *Science (80-.).* **1991**, *253* (5019), 542–545. https://doi.org/10.1126/science.253.5019.542.

(36) Weinberg, W. H.; Sun, Y. Quantification of Primary and Tertiary C-H Bond Cleavage in Alkaline Activation: Isobutane Dissociation on Pt(110)-(1 Sx 2). *Surf. Sci. Lett.* **1992**, *277* (1–2), L39–L46. https://doi.org/10.1016/0167-2584(92)90108-H.

(37) Kelly, D.; Weinberg, W. H. Isotope Effects in Trapping-mediated Chemisorption of Ethane and Propane on Ir(110). *J. Chem. Phys.* **1996**, *105* (9), 3789–3793. https://doi.org/10.1063/1.472199.

(38) Studt, F.; Sharafutdinov, I.; Abild-Pedersen, F.; Elkjær, C. F.; Hummelshøj, J. S.; Dahl, S.; Chorkendorff, I.; Nørskov, J. K. Discovery of a Ni-Ga Catalyst for Carbon Dioxide Reduction to Methanol. *Nat. Chem.* **2014**, *6* (4), 320–324. https://doi.org/10.1038/nchem.1873.

(39) Greeley, J. Theoretical Heterogeneous Catalysis: Scaling Relationships and Computational Catalyst Design. *Annu. Rev. Chem. Biomol. Eng.* **2016**, 7 (1), 605–635. https://doi.org/10.1146/annurev-chembioeng-080615-034413.

(40) Pérez-Ramírez, J.; López, N. Strategies to Break Linear Scaling Relationships. *Nat. Catal.* **2019**, *2* (11), 971–976. https://doi.org/10.1038/s41929-019-0376-6.

(41) Zhao, Z.; Liu, S.; Zha, S.; Cheng, D.; Studt, F.; Henkelman, G.; Gong, J. Theory-Guided Design of Catalytic Materials Using Scaling Relationships and Reactivity Descriptors. *Nat. Rev. Mater.* **2019**, *4* (12), 792–804. https://doi.org/10.1038/s41578-019-0152-x.

(42) Darby, M. T.; Stamatakis, M.; Michaelides, A.; Sykes,

E. C. H. Lonely Atoms with Special Gifts: Breaking Linear Scaling Relationships in Heterogeneous Catalysis with Single-Atom Alloys. *J. Phys. Chem. Lett.* **2018**, *9* (18), 5636–5646. https://doi.org/10.1021/acs.jpclett.8b01888.

(43) Bronsted, J. N. Acid and Basic Catalysis. *Chem. Rev.* **1928**, *5* (3), 231–338. https://doi.org/10.1021/cr60019a001.

(44) Evans, M. G.; Polanyi, M. Inertia and Driving Force of Chemical Reactions. *Trans. Faraday Soc.* **1938**, *34*, 11. https://doi.org/10.1039/tf9383400011.

(45) Pallassana, V.; Neurock, M. Electronic Factors Governing Ethylene Hydrogenation and Dehydrogenation Activity of Pseudomorphic PdML/Re(0001), PdML/Ru(0001), Pd(111), and PdML/Au(111) Surfaces. *J. Catal.* **2000**, *191* (2), 301–317. https://doi.org/10.1006/jcat.1999.2724.

(46) Liu, Z.-P.; Hu, P. General Trends in CO Dissociation on Transition Metal Surfaces. *J. Chem. Phys.* **2001**, *114* (19), 8244–8247. https://doi.org/10.1063/1.1372512.

(47) Logadottir, A.; Rod, T. .; Nørskov, J. .; Hammer, B.; Dahl, S.; Jacobsen, C. J. . The Brønsted–Evans–Polanyi Relation and the Volcano Plot for Ammonia Synthesis over Transition Metal Catalysts. *J. Catal.* **2001**, *197* (2), 229–231. https://doi.org/10.1006/jcat.2000.3087.

(48) Nørskov, J. K.; Bligaard, T.; Logadottir, A.; Bahn, S.; Hansen, L. B.; Bollinger, M.; Bengaard, H.; Hammer, B.; Sljivancanin, Z.; Mavrikakis, M.; et al. Universality in Heterogeneous Catalysis. *J. Catal.* **2002**, *209* (2), 275–278. https://doi.org/10.1006/jcat.2002.3615.

(49) Michaelides, A.; Liu, Z.-P.; Zhang, C. J.; Alavi, A.; King, D. A.; Hu, P. Identification of General Linear Relationships between Activation Energies and Enthalpy Changes for Dissociation Reactions at Surfaces. *J. Am. Chem. Soc.* **2003**, *125* (13), 3704–3705. https://doi.org/10.1021/ja027366r.

(50) Abild-Pedersen, F.; Greeley, J.; Studt, F.; Rossmeisl, J.; Munter, T. R.; Moses, P. G.; Skúlason, E.; Bligaard, T.; Nørskov, J. K. Scaling Properties of Adsorption Energies for Hydrogen-Containing Molecules on Transition-Metal Surfaces. *Phys. Rev. Lett.* **2007**, *99* (1), 016105. https://doi.org/10.1103/PhysRevLett.99.016105.

(51) Wang, S.; Temel, B.; Shen, J.; Jones, G.; Grabow, L. C.; Studt, F.; Bligaard, T.; Abild-Pedersen, F.; Christensen, C. H.; Nørskov, J. K. Universal Brønsted-Evans-Polanyi Relations for C–C, C–O, C–N, N–O, N–N, and O–O Dissociation Reactions. *Catal. Letters* **2011**, *141* (3), 370–373. https://doi.org/10.1007/s10562-010-0477-y.

(52) Crawford, P.; McAllister, B.; Hu, P. Insights into the Staggered Nature of Hydrogenation Reactivity over the 4d Transition Metals. *J. Phys. Chem. C* **2009**, *113* (13), 5222–5227. https://doi.org/10.1021/jp805244k.

(53) Wang, S.; Petzold, V.; Tripkovic, V.; Kleis, J.; Howalt, J. G.; Skúlason, E.; Fernández, E. M.; Hvolbæk, B.; Jones, G.; Toftelund, A.; et al. Universal Transition State Scaling Relations for (de)Hydrogenation over Transition Metals. *Phys. Chem. Chem. Phys.* **2011**, *13* (46), 20760. https://doi.org/10.1039/c1cp20547a.

(54) Xing, B.; Pang, X.-Y.; Wang, G.-C. C–H Bond Activation of Methane on Clean and Oxygen Pre-Covered Metals: A Systematic Theoretical Study. *J. Catal.* **2011**, *282* (1), 74–82. https://doi.org/10.1016/j.jcat.2011.05.027.

(55) Xing, B.; Wang, G.-C. Insight into the General Rule for the Activation of the X–H Bonds (X = C, N, O, S) Induced by Chemisorbed Oxygen Atoms. *Phys. Chem. Chem. Phys.* **2014**, *16* (6), 2621. https://doi.org/10.1039/c3cp53801j.

(56) Yoo, J. S.; Khan, T. S.; Abild-Pedersen, F.; Nørskov, J. K.; Studt, F. On the Role of the Surface Oxygen Species during A–H (A = C, N, O) Bond Activation: A Density Functional Theory Study. *Chem. Commun.* **2015**, *51* (13), 2621–

2624. https://doi.org/10.1039/C4CC08658A.

(57) Tsai, C.; Latimer, A. A.; Yoo, J. S.; Studt, F.; Abild-Pedersen, F. Predicting Promoter-Induced Bond Activation on Solid Catalysts Using Elementary Bond Orders. *J. Phys. Chem. Lett.* **2015**, *6* (18), 3670–3674. https://doi.org/10.1021/acs.jpclett.5b01792.

(58) Hibbitts, D.; Neurock, M. Promotional Effects of Chemisorbed Oxygen and Hydroxide in the Activation of C–H and O–H Bonds over Transition Metal Surfaces. *Surf. Sci.* **2016**, *650*, 210–220. https://doi.org/10.1016/j.susc.2016.01.012.

(59) Latimer, A. A.; Kulkarni, A. R.; Aljama, H.; Montoya, J. H.; Yoo, J. S.; Tsai, C.; Abild-Pedersen, F.; Studt, F.; Nørskov, J. K. Understanding Trends in C–H Bond Activation in Heterogeneous Catalysis. *Nat. Mater.* **2017**, *16* (2), 225–229. https://doi.org/10.1038/nmat4760.

(60) Yu, L.; Vilella, L.; Abild-Pedersen, F. Generic Approach to Access Barriers in Dehydrogenation Reactions. *Commun. Chem.* **2018**, *1* (1), 2. https://doi.org/10.1038/s42004-017-0001-z.

(61) Darby, M. T.; Réocreux, R.; Sykes, E. C. H.; Michaelides, A.; Stamatakis, M. Elucidating the Stability

and Reactivity of Surface Intermediates on Single-Atom Alloy Catalysts. *ACS Catal.* **2018**, *8* (6), 5038–5050. https://doi.org/10.1021/acscatal.8b00881.

(62) Sun, G.; Zhao, Z.-J.; Mu, R.; Zha, S.; Li, L.; Chen, S.; Zang, K.; Luo, J.; Li, Z.; Purdy, S. C.; et al. Breaking the Scaling Relationship via Thermally Stable Pt/Cu Single Atom Alloys for Catalytic Dehydrogenation. *Nat. Commun.* **2018**, *9* (1), 4454. https://doi.org/10.1038/s41467-018-06967-8.

(63) Kresse, G.; Furthmüller, J. Efficient Iterative Schemes for Ab Initio Total-Energy Calculations Using a Plane-Wave Basis Set. *Phys. Rev. B* **1996**, *54* (16), 11169–11186. https://doi.org/10.1103/PhysRevB.54.11169.

(64) Kresse, G.; Furthmüller, J. Efficiency of Ab-Initio Total Energy Calculations for Metals and Semiconductors Using a Plane-Wave Basis Set. *Comput. Mater. Sci.* **1996**, *6* (1), 15–50. https://doi.org/10.1016/0927-0256(96)00008-0.

(65) Hjorth Larsen, A.; Jørgen Mortensen, J.; Blomqvist, J.; Castelli, I. E.; Christensen, R.; Dułak, M.; Friis, J.; Groves, M. N.; Hammer, B.; Hargus, C.; et al. The Atomic Simulation Environment—a Python Library for Working with Atoms. *J. Phys. Condens. Matter* **2017**, *29* (27), 273002.

https://doi.org/10.1088/1361-648X/aa680e.

(66) Mortensen, J. J.; Kaasbjerg, K.; Frederiksen, S. L.; Nørskov, J. K.; Sethna, J. P.; Jacobsen, K. W. Bayesian Error Estimation in Density-Functional Theory. *Phys. Rev. Lett.* **2005**, *95* (21), 216401. https://doi.org/10.1103/PhysRevLett.95.216401.

(67) Wellendorff, J.; Lundgaard, K. T.; Møgelhøj, A.; Petzold, V.; Landis, D. D.; Nørskov, J. K.; Bligaard, T.; Jacobsen, K. W. Density Functionals for Surface Science: Exchange-Correlation Model Development with Bayesian Error Estimation. *Phys. Rev. B* **2012**, *85* (23), 235149. https://doi.org/10.1103/PhysRevB.85.235149.

(68) Blöchl, P. E. Projector Augmented-Wave Method. *Phys. Rev. B* **1994**, *50* (24), 17953–17979. https://doi.org/10.1103/PhysRevB.50.17953.

(69) Kresse, G.; Joubert, D. From Ultrasoft Pseudopotentials to the Projector Augmented-Wave Method. *Phys. Rev. B* **1999**, *59* (3), 1758–1775. https://doi.org/10.1103/PhysRevB.59.1758.

(70) Wellendorff, J.; Silbaugh, T. L.; Garcia-Pintos, D.; Nørskov, J. K.; Bligaard, T.; Studt, F.; Campbell, C. T. A Benchmark Database for Adsorption Bond Energies to

Transition Metal Surfaces and Comparison to Selected DFT Functionals. *Surf. Sci.* **2015**, *640*, 36–44. https://doi.org/10.1016/j.susc.2015.03.023.

(71) Mallikarjun Sharada, S.; Bligaard, T.; Luntz, A. C.; Kroes, G.-J.; Nørskov, J. K. SBH10: A Benchmark Database of Barrier Heights on Transition Metal Surfaces. *J. Phys. Chem. C* **2017**, *121* (36), 19807–19815. https://doi.org/10.1021/acs.jpcc.7b05677.

(72) Perdew, J. P.; Burke, K.; Ernzerhof, M. Generalized Gradient Approximation Made Simple. *Phys. Rev. Lett.* **1996**, *77* (18), 3865–3868. https://doi.org/10.1103/PhysRevLett.77.3865.

(73) Grimme, S.; Antony, J.; Ehrlich, S.; Krieg, H. A Consistent and Accurate Ab Initio Parametrization of Density Functional Dispersion Correction (DFT-D) for the 94 Elements H-Pu. *J. Chem. Phys.* **2010**, *132* (15), 154104. https://doi.org/10.1063/1.3382344.

(74) Henkelman, G.; Jónsson, H. Improved Tangent Estimate in the Nudged Elastic Band Method for Finding Minimum Energy Paths and Saddle Points. *J. Chem. Phys.* **2000**, *113* (22), 9978–9985. https://doi.org/10.1063/1.1323224.

(75) Henkelman, G.; Jónsson, H. A Dimer Method for Finding

Saddle Points on High Dimensional Potential Surfaces Using Only First Derivatives. *J. Chem. Phys.* **1999**, *111* (15), 7010–7022. https://doi.org/10.1063/1.480097.

(76) Toch, K.; Thybaut, J. W.; Marin, G. B. A Systematic Methodology for Kinetic Modeling of Chemical Reactions Applied to N-Hexane Hydroisomerization. *AIChE J.* **2015**, *61* (3), 880–892. https://doi.org/10.1002/aic.14680.

(77) Chen, Y.; Vlachos, D. G. Hydrogenation of Ethylene and Dehydrogenation and Hydrogenolysis of Ethane on Pt(111) and Pt(211): A Density Functional Theory Study. *J. Phys. Chem. C* **2010**, *114* (11), 4973–4982. https://doi.org/10.1021/jp909163z.

(78) Peng, G.; Gerceker, D.; Kumbhalkar, M.; Dumesic, J. A.; Mavrikakis, M. Ethane Dehydrogenation on Pristine and AlO x Decorated Pt Stepped Surfaces. *Catal. Sci. Technol.* **2018**, *8* (8), 2159–2174. https://doi.org/10.1039/C8CY00398J.

(79) Xu, L.; Stangland, E. E.; Mavrikakis, M. Ethylene versus Ethane: A DFT-Based Selectivity Descriptor for Efficient Catalyst Screening. *J. Catal.* **2018**, *362*, 18–24. https://doi.org/10.1016/j.jcat.2018.03.019.

(80) Vang, R. T.; Honkala, K.; Dahl, S.; Vestergaard, E. K.; Schnadt, J.; Lægsgaard, E.; Clausen, B. S.; Nørskov, J.

K.; Besenbacher, F. Ethylene Dissociation on Flat and Stepped Ni(111): A Combined STM and DFT Study. *Surf. Sci.* **2006**, *600* (1), 66–77. https://doi.org/10.1016/j.susc.2005.10.006.

(81) Lejaeghere, K.; Bihlmayer, G.; Blaha, P.; Bl, S.; Blum, V.; Caliste, D.; Castelli, I. E.; Clark, S. J.; Corso, A. D.; Gironcoli, S. De; et al. Reproducibility in Density-Functional Theory Calculations of Solids. *Science (80-.).* **2016**, *351* (6280), 1–11. https://doi.org/10.1126/science.aad3000.

(82) Hammer, B.; Hansen, L. B.; Nørskov, J. K. Improved Adsorption Energetics within Density-Functional Theory Using Revised Perdew-Burke-Ernzerhof Functionals. *Phys. Rev. B* **1999**, *59* (11), 7413–7421. https://doi.org/10.1103/PhysRevB.59.7413.

TOC Graphic

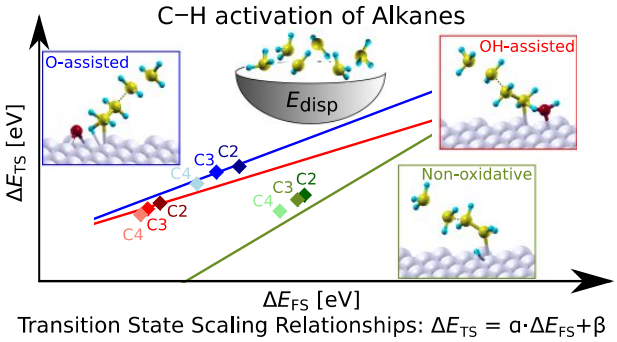

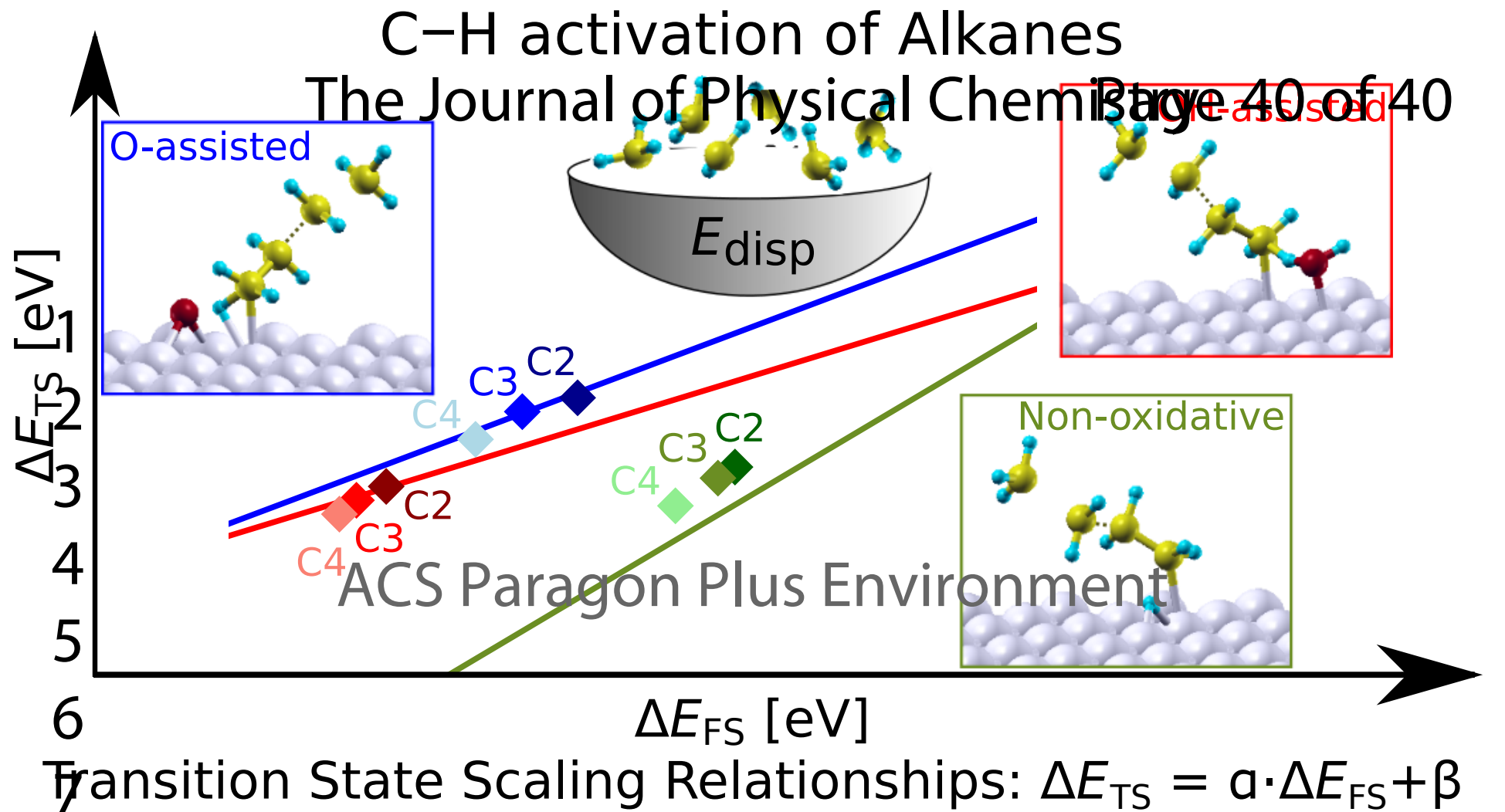

Transition State Scaling Relationships: $\Delta E_{TS} = \alpha \cdot \Delta E_{FS} + \beta$